Increasing Electrical Stimulation Efficacy in Degenerated Retina: Stimulus Waveform Design in a Multiscale Computational Model

Kyle Loizos, *Member, IEEE*, Robert Marc, Mark Humayun, *Fellow, IEEE*, James R. Anderson, Bryan W. Jones, and Gianluca Lazzi, *Fellow, IEEE*

***Abstract*— A computational model of electrical stimulation of the retina is proposed for investigating current waveforms used in prosthetic devices for restoring partial vision lost to retinal degenerative diseases. The model framework combines a connectome-based neural network model characterized by accurate morphological and synaptic properties with an admittance method model of bulk tissue and prosthetic electronics. In this model, the retina was computationally "degenerated," considering cellular death and anatomical changes that occur early in disease, as well as altered neural behavior that develops throughout the neurodegeneration and is likely interfering with current attempts at restoring vision. A resulting analysis of stimulation range and threshold of ON ganglion cells within the retina that are either healthy or in beginning stages of degeneration is presented for currently used stimulation waveforms, and an asymmetric biphasic current stimulation for subduing spontaneous firing to allow increased control over ganglion cell firing patterns in degenerated retina is proposed. Results show that stimulation thresholds of retinal ganglion cells do not notably vary after beginning stages of retina degeneration. In addition, simulation of proposed asymmetric waveforms showed the ability to enhance the control of ganglion cell firing via electrical stimulation.**

***Index Terms*— Retinal prosthesis, admittance method, multi-scale modeling, connectome, electrical stimulation.**

I. Introduction

RETINA prosthetic devices that use electrical stimulation have been designed in an attempt to restore some vision in patients with degenerative diseases, such as retinitis pigmentosa (RP) or age-related macular degeneration (AMD). These devices function by using electrodes to stimulate local regions of retina tissue, approximating spatiotemporal patterns for representing the image facing the patient. This has proven effective and has led to the design of multiple different prosthetic devices, as reviewed by Weiland [1]. Various devices are either employed in trials or have been recently commercialized. Most notably, the Argus II by Second Sight Medical Products Inc. (Sylmar, CA) in clinical trials provided subjects with sufficient visual perception to recognize objects and discern some letters of the alphabet. However, the best measured acuity is (20/1260) and only 55% of the individual electrodes have been able to provoke a light perception within safety limits. This implies that a single electrode is unable to locally stimulate cells and requires contribution from adjacent electrodes to cause stimulation [1]. With an array that has 60 electrodes, this further limits the already limited resolution. While the current implementations are encouraging and can provide an invaluable increase in functional vision to blind subjects [2], [3], strategies for improvement should be investigated.

Research has been conducted in an attempt to improve the efficiency and effectiveness of the stimulus waveform, considering shapes for decreasing the required injected current magnitude [4], [5], or precisely recreating desired spiking rates in retinal ganglion cells [6]. Attempts have been made to design clever waveforms for focusing current to locations on the array away from the electrodes [7]–[9], allowing for more stimulating sites on an array without requiring additional electrodes or drivers, and for selectively stimulating different cell types [10]–[14]. Additionally, studies of the electrodes themselves have considered the impact of the electrode size, placement, geometry, or the site of activation [15]–[18].

Properties of neural degeneration are clinically relevant and important to include in computational approaches for improving rehabilitative techniques. In clinical trials, stimulation thresholds have been well documented to increase with the severity of retinal degeneration, and there is significant literature towards understanding the reasons behind it. It has been observed that the location of the electrode (epi- or sub-retinal) and the severity of neural degeneration affect the resulting response to electrical stimulation, both in stimulation

Manuscript received February 7, 2017; revised September 3, 2017; accepted February 20, 2018. Date of publication May 1, 2018; date of current version June 6, 2018. This work was supported in part by the National Institute of the General Medical Sciences, National Institutes of Health, under Grant 1U01GM104604-01, in part by the National Institutes of Health under Grant EY02576 REM, Grant EY015128 REM/BWJ, and Grant EY014800 REM, in part by the National Science Foundation under Grant 0941717 REM/BWJ, in part by the Edward N. and Della L. Thome Memorial Foundation (BWJ), and in part by the Research to Prevent Blindness (REM/BWJ/MH). *(Corresponding author: Kyle Loizos.)*

K. Loizos and G. Lazzi are with the Department of Electrical and Computer Engineering, University of Utah, Salt Lake City, UT 84112 USA (e-mail: k.loizos@utah.edu).

R. Marc, J. R. Anderson, and B. W. Jones are with the John A. Moran Eye Center, University of Utah School of Medicine, Salt Lake City, UT 84112 USA.

M. Humayun is with the Departments of Ophthalmology and Biomedical Engineering, University of Southern California, Los Angeles, CA 90033 USA.

Digital Object Identifier 10.1109/TNSRE.2018.2832055

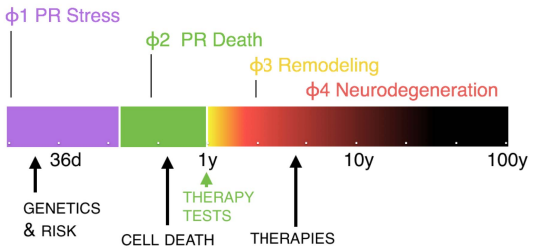

Fig. 1. Diagram of the timeline of retina degeneration.

range and threshold [19]. In studies using animal models of degeneration, stimulation thresholds for indirect activation, presynaptic to retinal ganglion cells, have been observed to increase [20]–[23]. However, in the case that retinal ganglion cells are directly stimulated, the retina remains responsive [24]. Note that indirect stimulation is still possible post photoreceptor degeneration, but requires increased injected charge [22], [23]. In a study of the electrophysiological effects of degenerating retina, it was found that by pharmacologically inhibiting synapses, spontaneous activity in retinal ganglion cells was altered. This occurred for both control and P23H rats (a model of autosomal dominant RP), implying that retinal circuitry remains at least partially intact after photoreceptor degeneration, and further supports the possibility of indirect ganglion cell stimulation [25]. In fact, Weitz *et al.* [26] have shown the utilization of increased pulse duration for stimulating inner neural circuitry to achieve a higher level of focus of the resulting light response in clinical trials.

Using a Tg P347L rabbit (an animal model of human dominant RP), which has a lifespan four times longer than a mouse, has shown that retinal remodeling is relentlessly progressive, continuing until greater than 90% of neurons are gone [27]. The timeline of degeneration can be broken down into 4 phases, as shown in the diagram in Fig. 1. Throughout the first two phases, up to a year in the rabbit model, photoreceptors are stressed and cellular death occurs. This can be addressed in computational models by disregarding photoreceptors completely and either considering direct stimulation of ganglion cells or indirect stimulation of ganglion cells through the stimulation of presynaptic circuitry, as is done for example in [14], [28], and [29]. However, photoreceptor death does not mark the end of the disease, occurs early on, and has electrophysiological effects beyond photoreceptors no longer providing light-induced input to retina circuitry. As disease progresses towards patients becoming completely blind, there is extensive remodeling of the retina, including cell migration and spontaneous neural activity [30], [31]. During this remodeling phase of degeneration, spontaneous firing and oscillatory behavior has been observed in the surviving neural networks [32]–[34]. Thus, removing the input from light-sensitive cells does not remove neural activity in the retina, and instead alters it. One source of spontaneous activity is believed to be the coupling between AII amacrine and cone bipolar cells [35], [36]. The lack of presynaptic input from the now-degenerated photoreceptors, leads to oscillatory membrane voltage in the coupled AII and cone bipolar cells and subsequent phasic bursting in ganglion cells. Studies have shown that blocking gap junctions can eliminate such activity, helping to validate this claim [33], [37]. Such alterations in ganglion cell physiology in degenerating retina, and change in rates of spontaneous activity, have been shown to affect the responsiveness to electrical stimulation [38]–[40]. This could be sufficient to interrupt attempts at systematic electrical stimulation for restoring vision.

Towards improving the efficacy of the electrical stimulation, we provide a simulation framework for understanding the response of degenerating retina to currently used electrical stimuli and for designing new electrode geometries and stimuli waveforms. This framework is based on a multiscale multiphysics platform, using the Admittance Method for computing the electric field within a model of tissue [41], and NEURON [42] for simulating the resulting response in a neural network, following the authors' previous work [43]. Briefly, the Admittance Method is a quasi-static electromagnetic field solver. In this method, a voxelized model that is discretized by tissue/material dielectric properties is first constructed. It takes as input the admittance between each node in the model and a set of current sources. A set of linear equations is constructed, and an iterative solver is used to compute the voltage at each node in the model. Further detail on the methodology are provided in [41] and [44].

From a connectomics dataset [45], a model of a ganglion cell network, consisting of realistic cellular morphology and synaptic type, distribution, and weight is constructed in NEURON. Biophysical data from literature were incorporated in each individual cell, and a script for applying the extracellular electric field from Admittance Method simulations to observe resulting network and cellular behavior to a given input was written. To induce spontaneous neural activity indicative of degenerated retina, the intrinsic properties of AII amacrine cells within this model were altered to produce an oscillatory membrane potential, following Choi *et al.* [37]. Translating a connectome dataset to a computational model is a uniquely qualified approach for this study, as it is comprised of real imaged morphology and observed connections that allows for as accurate as possible of a representation of a retina neural network and resultant network behavior, reducing the need for assumptions regarding interconnectivity. This serves as a tool for further considering cellular death within the inner plexiform layer by "degenerating" the computational retina and decreasing the strength of individual synapses or gap junctions, and number of cells.

At a larger spatial scale, a model of bulk tissue and prosthetic electronics was constructed using the Admittance Method, which was used to compute extracellular electric field due to anatomical changes in early stages of degeneration. Coupling this Admittance Method model of extracellular space with the connectome-based NEURON model combines the ability to change the anatomical structure of the retina, integrate implant electronics, and alter the biophysical properties of the cells and interconnectivity to virtually degenerate the retina.

This leads to the most detailed modeling framework for studying electrical stimulation of degenerated retina to date, effectively coupling decades of research of retina stimulation,

including electrophysiological studies of cellular behavior, the connectivity map from connectomics, geometrical and electrical features of prosthetic electrode arrays, clinical and experimental data on degeneration of retina, and computational electromagnetics into a single simulation platform. In this paper, stimulation threshold and range are computed for varying degrees of degeneration and neural network complexity, and a stimulation waveform that reduces spontaneous activity within a degenerated retina and provides more effective control over ganglion cell stimulation is proposed.

II. Methods

A. Constructing Model of Bulk Retina Tissue and Electronics

To simulate the extracellular electric field due to an applied current stimulus, a discretized bulk-tissue level model of retina tissue and a prosthetic electrode array was constructed using in-house software. A section of retina tissue, with dimensions of 6.25 mm $\times$ 4.25 mm was described as layers of homogeneous medium, following the anatomy of healthy mammalian retina. It was voxelized with a resolution of 10 μm and discretized based on bulk tissue resistivity. For the inner band, including the ganglion cell layer, inner plexiform layer, and inner nuclear layer, the resistivity and layer thickness were given properties that were assigned using knowledge of the cellular morphology, applying values reported in [43]. In this method, the morphological data from the connectome dataset that was translated to a NEURON model for this study, as discussed in the next section, was voxelized and segmented into these three retina layers. Electrodes were placed on either side of the tissue. The Admittance Method [41], [44] was then used to apply a current source through the tissue, and the voltage across the electrodes was computed and used to calculate the resistivity. This was using morphology from the exact connectome dataset used in this study, making these effective resistivity values for bulk tissue as precise as possible for considering stimulation of this cellular network. The middle band, including the photoreceptor and outer plexiform layers was lumped into a single layer, applying properties reported for retina tissue [46], and the pigment epithelium, choroid, and sclera were given properties as reported by Gabriel [46]. The resistivity and layer thickness are reported in Table 1. A 6×10 array of 200 μm electrodes was placed epi-retinally, against the retina surface. The electrodes were given resistivity of platinum (10.6×10^{-8} Ω m), which were considered flush with insulating material, given resistivity of 10^{7} Ω m. A rendering of the model is shown in Fig. 2. For simulating resulting voltage throughout this model for one or more of the electrodes injecting current, a multi-resolution Admittance Method [41] was used, following [28].

This model was then modified to take into account anatomical changes that occur during early stages of degenerative disease, shrinking the middle band of the retina considerably, and mildly shrinking the inner band, following measurements from rat retina before and after photoreceptor degeneration from [47]. The resulting layer thickness is provided in Table 1.

TABLE I
Retina Layer Discretization

Layer	Resistivity (Ω m)	Layer Thickness Healthy (μm)	Layer Thickness Degenerated (μm)
Vitreous	0.667	-	-
GCL	0.912	50	40
IPL	2.43	30	30
INL	0.97	50	30
OPL and ONL	1.98	150	30
PE	3200	10	10
Choroid/Sclera	1.98	-	-

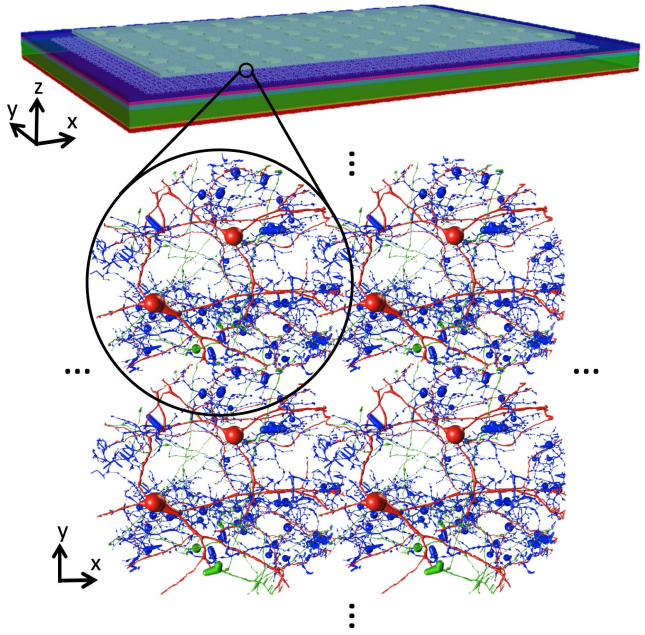

Fig. 2. Diagram of the multi-scale model of electrical stimulation of retinal tissue, including (Top) a discretized Admittance Method model consisting of a layered structure describing the retina and a 6×10 electrode array placed 0.05 mm away from the retina surface, and (bottom) a rendering of the NEURON model of an ON ganglion cell network, which was tiled to populate the entire ganglion cell, inner plexiform, and bipolar cell layers beneath the electrode array. This resulted in 888 cellular networks, each simulated independently.

B. Translating Retina Connectome to Neuron Model

Morphological data for a neural network extracted from a connectome dataset of rabbit retina was converted into SWC format for importing to NEURON software [42] as a compartmentalized model, following the authors' previous work [28], [43]. This connectome is basically a connectivity map originating from transmission electron microscopy (TEM) images of rabbit retina, that has been manually annotated to populate a dataset containing morphology, cell type, receptor distribution and type, etc. [48] The extracted network used in this study consists of an ON transient ganglion cell and every cell that it directly communicates with, considering a total of 117 cells that are either ganglion, cone bipolar, or inhibitory amacrine cells. A rendering of the morphology of this cellular network is given in Fig. 2, and a map of the connectivity of

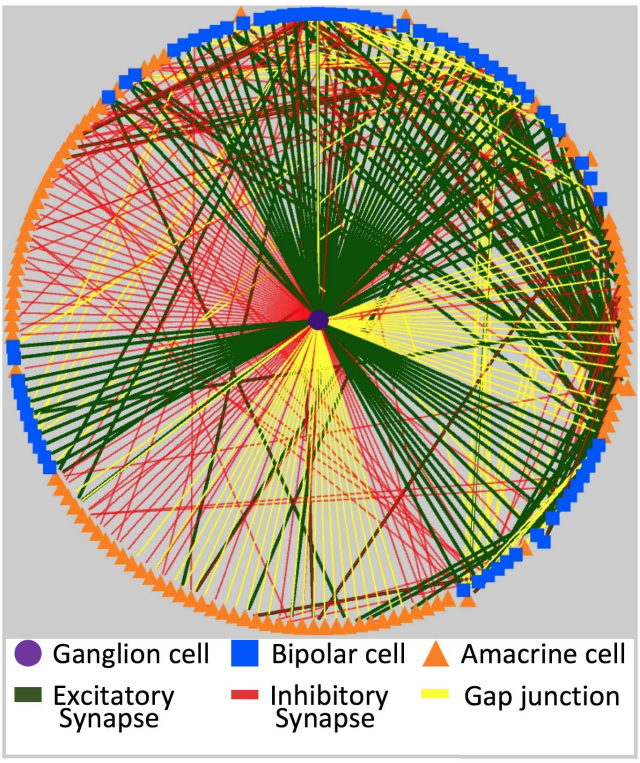

Fig. 3. Connectivity diagram of the neural network model, showing the ON ganglion cell considered in this study and every presynaptic cell (with the morphology depicted in Fig. 2), as extracted from the connectomics dataset. The node at the center is the ON ganglion cell and the nodes on the outside of the circular diagram are bipolar cells (blue) and amacrine cells (orange). The edges represent connections, including ribbon synapses (green), conventional synapses (red), and gap junctions (yellow).

this network is given in Fig. 3. This network model was then tiled to populate the entire inner band of retina within the Admittance Method model described in the previous section, filling the entire region beneath the electrode array to allow for simulating the stimulation range and threshold for given inputs. The center-to-center distance between adjacent cellular networks was set to 150 μm. This resulted in 888 cellular networks for a total of over 100k cells and 10.75 million compartments, as shown in the diagram in Fig. 2.

Biophysical properties from literature were added to each cell in the NEURON model in order to include the cellular response. This includes the five ionic channel model of Fohlmeister and Miller [49] and Fohlmeister [50] for the ganglion cells, a five ionic channel model for cone bipolar cells [51], [52], and a Hodgkin-Huxley model for the amacrine cells [52], with more detail provided in [43]. A complex ribbon synapse model was implemented for all ribbon synapses in the model [53], which did not provide any discernable difference in the stimulation threshold or range simulations from using a graded synapse model following that of Publio *et al.* [52]. Synapse conductance was weighted based on the area of the synaptic terminal, as observed during construction of the connectome dataset, taking the minimum area of the presynaptic and postsynaptic terminals. This resulted in the inclusion of over 500 projections within the model, including ribbon synapses, conventional synapses, and gap junctions. A diagram of all of the connections considered is provided in Fig. 3, providing a qualitative illustration of the extent of connectivity.

A script was written for extracting the location of the center of each compartment within the NEURON model, interpolating resulting voltage from Admittance Method simulations at these locations, and applying them as extracellular voltage sources using the 'extracellular' mechanism that is built in to NEURON, adding them in series with the membrane. This allowed for the simulation of the effects of electrical stimulation in realistic electrodes in heterogenous tissue on neural network behavior.

C. Impact of Anatomical Changes on Computational Results

1) Stimulation Threshold: The current magnitude stimulation threshold was computed for a single ganglion cell network for four cases: considering a single electrode firing and all electrodes firing to see any effects on threshold from using combined electrode stimulation for both anatomical models of retina tissue described in section II.A, considering retina before and after early degeneration by shrinking the layer thickness as shown in Table I. This was conducted for a stimulation waveform that is currently used in devices such as the Argus II as reported in literature [2], [54]: a 1 ms wide cathode-first biphasic pulse with a 1 ms interphase delay. The Admittance Method was used for calculating the voltage throughout the model for this waveform for a magnitude of 10 μA, applied at either one of the center electrodes or all 60 electrodes simultaneously. The result was interpolated and applied to the neural network that was centered beneath the single firing electrode.

A script was written in NEURON for then scaling the input linearly in order to find the stimulation threshold. It takes a guess for the range of scaling factors that would include the stimulation threshold as an input. The maximum is applied, scaling all extracellularly applied voltage in the model, and the NEURON simulation is run. If there is no action potential (defined by the membrane potential of the ganglion cell in the network exceeding 20mV), then this value is doubled until an action potential is observed, setting the previous value as the minimum of the starting range. This process is then repeated for the minimum value, cutting the scaling factor in half until no action potential is observed. The average of the two scaling factors is then attempted, and is set as either the new maximum (if resulting in an action potential) or the new minimum (if there is no action potential). This process is repeated until the difference between the maximum and minimum is less than a predefined residue (using 1 nA here).

It has been observed experimentally that stimulation threshold is higher in degenerated retina vs. healthy retina. Weiland [1] mention in their review that not considering indirect stimulation, there is likely no change in thresholds from healthy to degenerated retina, based on results by Sekirnjak *et al.* [24]. We explore this hypothesis here, considering the stimulation threshold with and without synaptic

connectivity in order to model direct and/or indirect stimulation of ganglion cells.

2) Stimulation Range: The range of stimulation from a single electrode in the center of the array was simulated by running Admittance Method simulation, with values guided by the resulting stimulation thresholds from the previous section. This study was conducted in a similar fashion, but considering a constant input, of either 75, 100, 125, or 150 μA, and applying the resulting voltage to all 888 cellular networks in the tiled retina model shown in Fig. 2.

D. Retina Degeneration - Spontaneous Activity

1) Inducing Spontaneous Firing: Oscillatory neural activity that arises from the coupling between AII amacrine and cone bipolar cells with lack of photoreceptor excitatory input was then added to the cellular network model [33], [35]. The model up to this point does not include AII cells, as the network extracted from the connectome only included an ON ganglion cell and the cells that directly communicate with it. So, the connectome was referenced again, noting each of the cone bipolar cells in this network coupled to an AII amacrine cell, finding 47 cells [55]. An AII model was built in NEURON, with morphology and intrinsic properties following exactly that of Choi *et al.* [37], including fast Na and slow M-type K conductances to create an oscillatory membrane potential that is seen in the experimental studies of Choi *et al.* [37]. Their model was constructed in MATLAB, so it was re-implemented in NEURON and coupled with the appropriate bipolar cells in the neural network model.

The results in their paper were first reconstructed, ensuring that for the same gap junction conductance between the AII and BCs that the same oscillating membrane voltage was achieved (matched frequency, magnitude, and offset voltage). In this study, the bipolar cell models were simplified to only include passive components as used in the study in Choi's paper. Excitatory synapses within the cellular network were added back into the model in order to see any phasic firing in the ganglion cells that result from this oscillatory activity in the coupled AII-BC network. This was done for a single AII and for all 47 AII cells. Inhibitory synapses and gap junctions existing in the network were then incorporated to study the effects neural connectivity may have on such behavior.

2) Stimulus Waveform Design to Address Spontaneous Activity: As shown in [37], a constant current source applied to the bipolar cells has the ability to eliminate oscillatory activity. This was repeated here to ensure that a sufficiently high current source would indeed eliminate spontaneous activity, and the magnitude of membrane potential was compared with that in [37] for various gap junction conductance. Then, an L-type Ca ionic channel was added back into the bipolar cells, due to it being a possible reason for bipolar cells responding to wide pulses while ganglion cells do not respond (as shown by Freeman *et al.* [10], [11], using low-frequency sinusoidal stimulation). Simulations from the previous section were repeated to ensure that this did not interfere with the oscillatory membrane potential of the coupled AII and cone bipolar cells, and resulting phasic bursting in the ganglion cell due to excitatory synaptic input from these bipolar cells.

Sinusoidal simulation was attempted, with the motive being the ability to selectively stimulate bipolar cells with low frequency sinusoidal stimulation (5-25 Hz), causing indirect stimulation [10], [11]. This was found to only induce spiking on the peaks of the sinusoids, effectively inducing the activity that is believed to already occur in the degenerating retina from these oscillatory membrane potential that is exhibited in bipolar cells from the coupling of AII to BC.

So, a biphasic pulse is revisited. A cathodic pulse that is tall and narrow (similar to what is currently used) is used to stimulate the ganglion cell, followed by a wide anodic pulse that is long enough that ganglion cells do not respond, but bipolar cells can be sufficiently stimulated to eliminate their oscillatory behavior. The magnitude of the waveforms are modified appropriately to ensure a charge balanced stimulus, using the stimulation thresholds from section 2.c.1 as a guideline for the cathodic pulse, and a minimum pulse width of 10ms for the anodic pulse, maintaining sufficiently wide pulses to not stimulate the ganglion cells while still eliminating the oscillatory behavior. This is based on the study by Freeman *et al.* [10], showing stimulation frequency of less than 100 Hz to not cause direct stimulation of ganglion cells.

This proposed waveform would allow control over ganglion cell firing, eliminating spontaneous bursts of action potentials in ganglion cells and only allowing action potentials when desired. In addition, this type of asymmetric biphasic pulse was also suggested as a more efficient waveform for retina stimulation, decreasing the total charge injection while maintaining stimulation, following a set of experimental studies given in [5].

III. Results

A. Stimulation Threshold

The resulting stimulation thresholds for the ganglion cell in this network shows that the lowest threshold is in the degenerated bulk tissue model with synaptic connectivity. This makes sense intuitively: by reducing the thickness of the retina, current density becomes higher within the inner layers of the retina, spreading through a larger range of tissue, and therefore reducing the stimulation threshold. Slices of the voltage profile through the firing electrode for both bulk tissue models are included in Fig. 4. to illustrate this point. Including synaptic activity also allows for the stimulation of presynaptic circuitry that can indirectly contribute to the stimulation of the ganglion cell. When synaptic activity is removed, considering only direct stimulation of the ganglion cells, the threshold increases. This leads to a similar stimulation threshold for the healthy anatomical model including synaptic activity and the degenerated anatomical model with loss of synaptic activity. This preliminary result supports Weiland's claim in [1] that by including indirect stimulation, the stimulation thresholds of ganglion cells do not vary by a notable amount between healthy and degenerated retina once the synaptic loss due to degeneration is considered. In addition, the stimulation threshold is reduced significantly by considering simultaneous current injection at all electrodes, as expected. A plot of these results is given in Fig. 5.

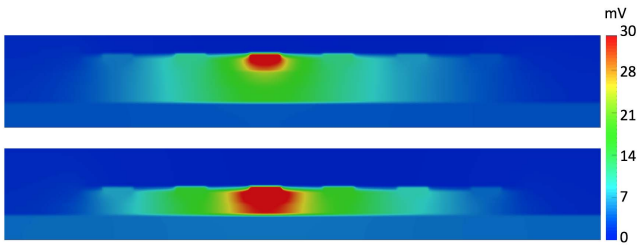

Fig. 4. Slice of the resulting voltage for a single electrode stimulation for a healthy retina (top) and degenerated retina (bottom).

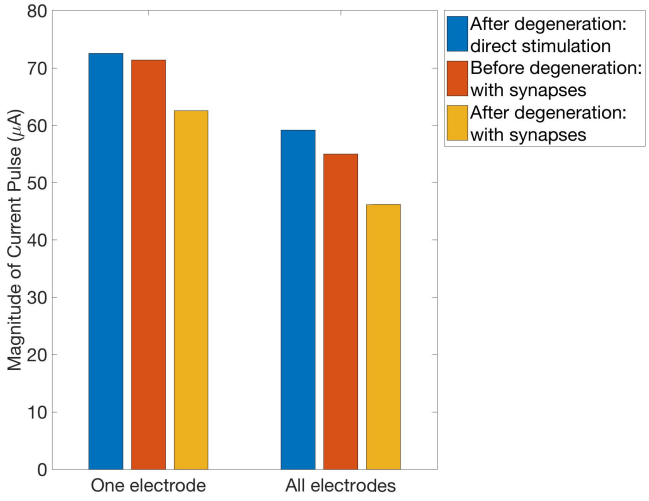

Fig. 5. Computed stimulation threshold for a given 1ms biphasic pulse for a single electrode, or simultaneous 60-electrode stimulation, considering direct and/or indirect stimulation for retina before and after early degeneration by considering modified retina layer thickness as given in Table I.

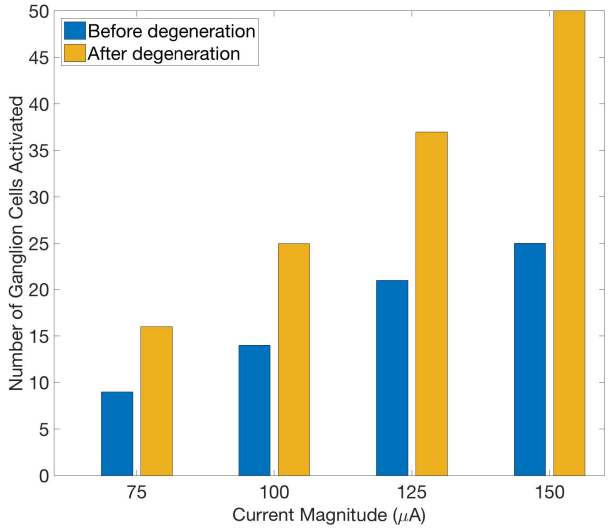

Fig. 6. Computed stimulation range of ganglion cells, providing the number of ganglion cells stimulated for varying current magnitude and a 1ms wide biphasic pulse.

B. Stimulation Range

Near the stimulation threshold computed in the previous section for direct stimulation of ganglion cells, considering a magnitude of 75 μA applied to a single electrode, a total of nine cells were activated for retina before degeneration and sixteen cells were activated after shrinking the thickness of retinal layers to represent beginning stages of degeneration. For increased current magnitude, the stimulation range increased, as expected. Fig. 6 shows the number of ganglion cells stimulated for increased current magnitude, reaching as many as 50 for the degenerated retina at a magnitude of 150 μA, which is within the range of current magnitude used in currently implanted patients [2].

C. Spontaneous Neural Activity Due to Retina Degeneration

The induced oscillatory membrane voltage in AII cells and passive cone bipolar cells (CBC) matched that of [37]. The response of a single coupled AII-CBC is shown in Fig. 7A. By adding excitatory synapses into the model, this oscillatory behavior led to phasic firing in the ganglion cell, with action potentials induced during the sinusoidal crests, as expected. When all 47 AII cells, and appropriate gap junctions with a conductance of 500 pS were included, there was a much higher firing rate during the bursts of ganglion cell activity, still during the crests of the sinusoids in the bipolar cells. Such activity can be tailored in this model by simply adjusting the gap junction conductance or number of cells that exhibit oscillatory behavior. By including inhibition and gap junctions in the network, the response is a bit more interesting, creating a more spontaneous pattern of ganglion cell stimulation, allowing for indirect stimulation to occur within some of the inhibitory networks in the connectome. Resulting ganglion cell membrane potential for these cases is provided in Fig. 7. As discussed by Abramian et al. [29], inhibition is important in understanding response to epiretinal electrical stimulation, as in can significantly impact spatial firing patterns, and should be included in computational efforts. In addition, gap junctions, active dendrites and coupling by electrical synapses is also important in order to consider dynamic range [52], [56]. Using this multiscale modeling platform, such features can be considered and altered, allowing for such observations of possible neural behavior in degenerating and electrically stimulated retina.

D. Stimulation Waveform Design

For designing stimuli for more effective stimulation, decreasing or eliminating spontaneous firing in ganglion cells in degenerating retina, the model in the previous section considering a single AII cell with oscillating membrane potential was considered. As mentioned, an applied constant-current stimuli can reduce oscillatory behavior in the coupled AII-CBC network sufficiently. This was tested, applying a current clamp with varying magnitude to the CBC with oscillating membrane voltage, finding above 20 pA to eliminate the low-frequency oscillatory behavior, matching results in [37]. In addition, when above 10 pA was applied, the resulting membrane potential offset and reduced oscillatory behavior was sufficient to completely eliminate spontaneous ganglion cell activity.

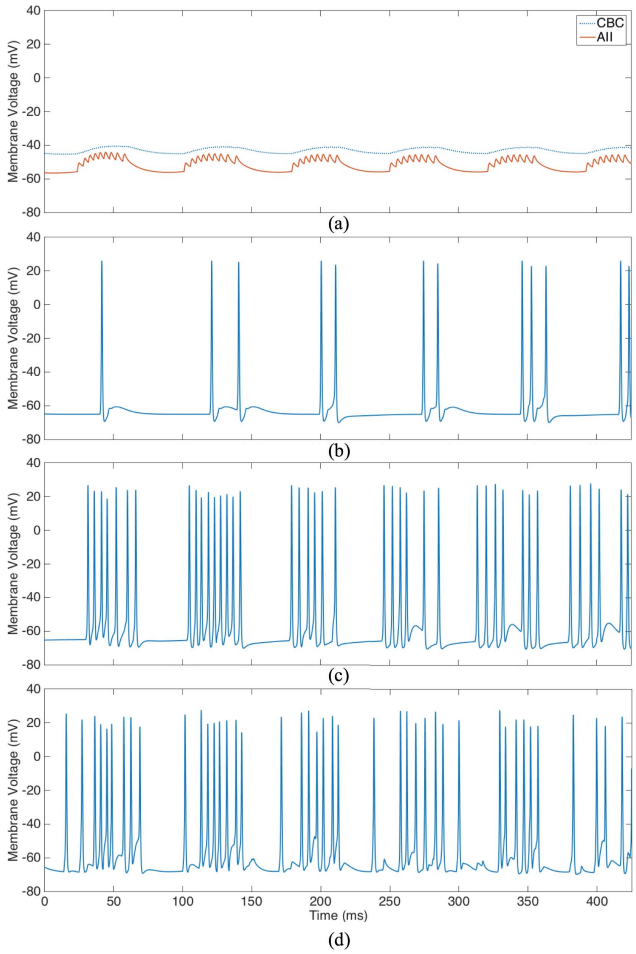

Fig. 7. Induced spontaneous activity in the retina neural network model without electrical stimulation intervention, showing the membrane potential for (a) a single cone bipolar cell coupled to an AII cell (reproduction of results in [37] with gap junction conductance of 500 pS); (b) ganglion cell that is post-synaptic to the bipolar cell in (a), showing induced spontaneous firing; (c) the same ganglion cell as plotted in (b), but with all 47 AII amacrine cells integrated into the model, coupled with CBC's appropriately via gap junctions, and all excitatory synapses included in the neural network model showing increased firing; and (d) the same as in (c) but with all excitatory and inhibitory synapses and gap junctions included in the neural network model, showing additional spontaneous activity.

The proposed waveform in this paper is to use asymmetric biphasic pulses for stimulating ganglion cells. Wide anodic pulses with low, sub-threshold magnitude can be used to eliminate unwanted ganglion cell stimulation for the duration of the pulse, and narrow, tall, supra-threshold cathodic pulses can be used to cause single ganglion cell action potentials. This allows for increased control over ganglion cell temporal spiking behavior, considering possible oscillatory behavior existing within subjects' degenerated retina.

To study this pulse shape, Admittance Method simulations were run for various pulse widths and magnitudes. An example waveform is shown in Fig. 8B, consisting of a width of 1 ms for the cathodic pulse with a magnitude of 75 μA, which is sufficient to cause stimulation as found in previous results in this paper. The anodic pulse has a width of 15 ms and magnitude of 5 μA, which is sufficiently long to stimulate the CBCs and reduce oscillatory membrane potential. An interphase gap of 1 ms was considered, which has been shown to increase the efficiency of currently-used biphasic stimuli [4] and is relevant to previous clinical trials [54]. The resulting voltage was applied to the neural network model as was done in previous sections, and the resulting ganglion cell membrane potential is shown in Fig. 8D. The result was as intended, with a single action potential in the ganglion cell occurring during direct stimulation by the cathodic pulse, while the spontaneous activity was subdued by the wide anodic pulse. This was then compared with a symmetric biphasic waveform, similar to as reported in clinical trials in [54]. In this case an identical cathodic pulse and interphase gap to the proposed waveform was used, followed by a 1ms-wide 75 μA anodic pulse. A plot of the waveform is provided in Fig. 8A and the resulting membrane potential of the ganglion cell is shown in Fig. 8C. In contrast to the result using the asymmetric waveform, multiple spikes are simulated after two of the five applied pulses.

In addition to this waveform shape effectively subduing spontaneous activity during electrical stimulation, it is favorable to safety considerations. Note that the anodic phase in both waveforms in Fig. 8 result in the same charge injection, maintaining a charge-balanced waveform in order to reduce irreversible electrochemical reactions at the electrode-tissue interface. By choosing the magnitude and duration of the cathodic and anodic pulses appropriately, a charge-balanced waveform is maintained and total charge density and charge per phase remain within safety limits, following criteria in [57] and [58]. However, the longer the anodic reversal phase, the more likely tissue damage will occur [59]. A similar risk results from an excessive interphase gap, due to the delay in reversing the direction of electrochemical reactions resulting from the cathodic phase. Care needs to be taken in designing the width of both the pulses and the interphase gap appropriately such that unrecoverable charge is not accumulated [59].

IV. Discussion

A. Neural Network Modeling

While this modeling effort provides a substantial number of parameters for controlling the extent of neural connectivity and how it may affect the response of retina to electrical stimulation, it has limited horizontal communication. In the simulations for computing the range of stimulation, in which neural networks are tiled into a single model, as shown in Fig. 2, each network acts independently. In reality, some of the cells in this neural network, including the ganglion cell and amacrine cells extend beyond the 0.25 mm diameter that the connectome used is limited to. Indeed, the ganglion cell dendritic arbor is likely about 0.5-0.7 mm in diameter [60]. In addition, there is horizontal communication across sheets of specific types of bipolar cells, horizontal or amacrine cells, gap junction-coupled ganglion cells, etc., all of which may affect the stimulation range that is reported in this computational study. This was limited in this study in an attempt to only include actually observed connectivity. Future expansion of

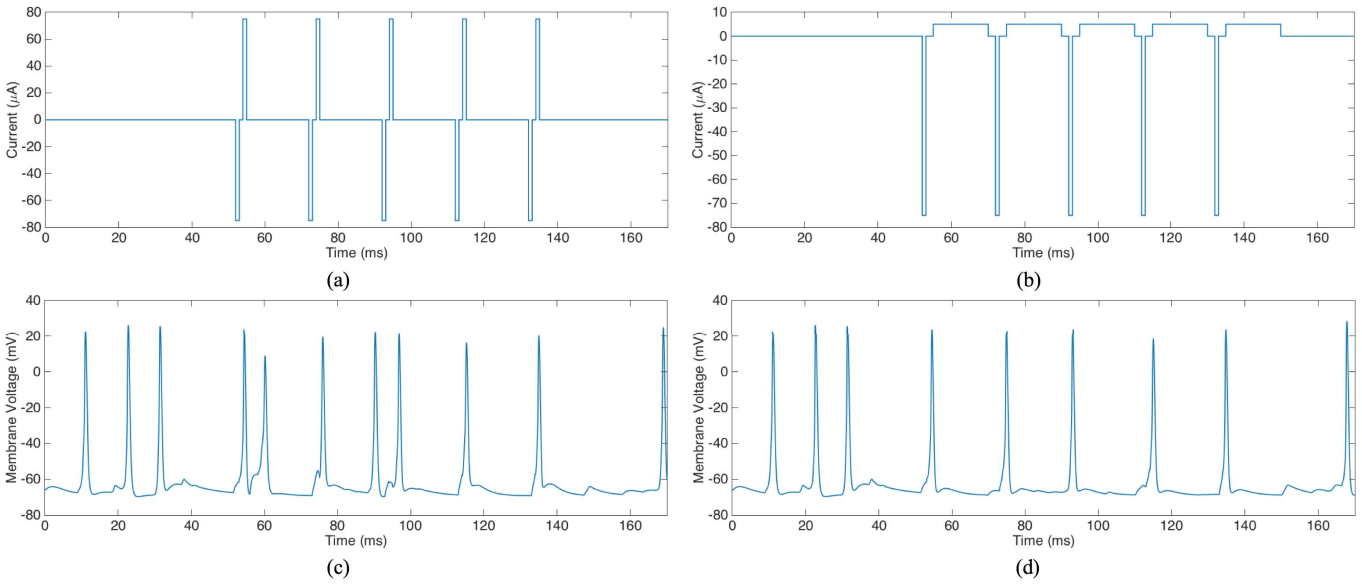

Fig. 8. Comparison of a symmetric and an asymmetric biphasic waveform. (a) Symmetric biphasic current stimulus applied in an Admittance Method simulation. (b) Asymmetric biphasic current stimulus applied in an Admittance Method simulation. (c) Simulated ganglion cell membrane voltage using the symmetric current stimulus shown in (a). (d) Simulated ganglion cell membrane voltage resulting from the asymmetric current stimulus shown in (b), illustrating ability to control spiking, eliminating spontaneous firing and limiting action potential to single firing at the time of cathodic pulse.

this modeling effort can be conducted for constructing a more accurate representation of retinal neural tissue.

B. Retina Degeneration

In addition to the neural network modeling limitations, the bulk tissue level models used for simulating extracellular voltage due to electrical stimulation maintains a layered structure for the retina. This is consistent with literature for early phases of degeneration, but does not extend to later phases, during which electrical stimulation prosthetic intervention is implemented. During the neural remodeling and continual neurodegeneration phases, there are substantial modifications to the retina anatomy, including cell migration, and cellular death that continues until nearly 90% of the cells are gone. This practically eliminates the structure of layered tissue with homogeneous electrical resistivity as seen here, as shown in Fig. 9, and calls for a more complex heterogeneous representation of the tissue.

In addition to the added spontaneous ganglion cell activity that is considered in this paper, there are further molecular reprogramming events during remodeling, including completely new connections, glutamate receptor revisions and altered Müller cell functionality [61]. None of such features are incorporated into the modeling structure as of yet, and consequences on attempted electrical stimulation is unknown. The modeling framework presented here has the ability to include all mentioned features, altering the heterogeneity of the tissue and network connectivity.

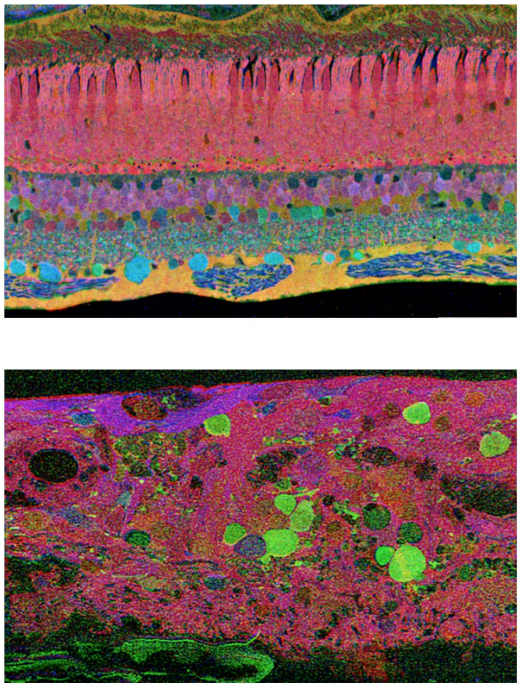

Fig. 9. Images of human retina, both before degeneration (top) and after extensive degeneration due to retinitis pigmentosa (bottom).

C. Electrode Design

Comparing with clinical data, the stimulation thresholds reported from this computational study are on the lower end of what has been observed. A reason for this is likely the location of the electrodes in this model. As discussed in [2] and [54], the distance between the retina surface and the electrode array can vary from patient to patient and can increase over time. This leads to an increased electrode impedance and stimulation threshold. This can certainly be considered in the modeling

framework provided in this paper to study how the electrode distance affects the stimulation threshold and range.

D. Implications for Clinical Applications

Currently the timing of implantation is late in disease, after patients have undergone years of disease and have become blind. As such, extensive retina remodeling and neurodegeneration has occurred by the time electrical stimulation rehabilitative techniques are attempted. This makes the proposed waveform in this paper highly clinically relevant, considering some spontaneous behavior that occurs during remodeling in the design of the waveform. As discussed by Weiland [1], only 55% of electrodes in current patients are effective independently. Applying the waveform proposed here, this number can hopefully increase. The simulation results in this paper show the potential of this waveform to subdue spontaneous activity in retinal ganglion cells that results from neural remodeling and neurodegeneration using the same energy as a comparable symmetric biphasic waveform. In doing so, control over the firing rate of ganglion cells is increased. Asymmetric biphasic pules have been considered in previous experimental studies [5], [62]. However, the ability to scale this to clinical application still needs to be investigated to validate added effectivity.

V. Conclusion

In this paper, a multiscale multiphysics computational framework for modeling electrical stimulation of degenerated retina was proposed. Using this framework, the effects of cellular network connectivity, anatomical changes, and spontaneous activity observed in degenerated retina on electrical stimulation attempts were investigated. This provided computed stimulation threshold and range of ganglion cells for varying degrees of degeneration. Through observations of such studies, a waveform shape with increased effectivity in degenerated retina was proposed, applying asymmetric biphasic pulses for reducing spontaneous neural activity and allowing increased control over the timing of ganglion cell action potentials. The authors hope for such results to increase the effectivity of currently-implanted devices, and for the proposed modeling framework to continue to provide understanding of retina neural behavior, how it changes during degenerative disease, and provide additional recommendation for further increased stimulation efficiency and efficacy in prosthetic devices for restoring vision.

References

[1] J. D. Weiland, "Retinal prosthesis," *Annu. Rev. Biomed. Eng.*, vol. 61, no. 5, pp. 24–1412, 2014.

[2] A. K. Ahuja *et al.*, "Factors affecting perceptual threshold in Argus II retinal prosthesis subjects," *Transl. Vis. Sci. Technol.*, vol. 2, p. 1, Apr. 2013. [Online]. Available: http://www.pubmedcentral.nih.gov/articlerender.fcgi?artid=3763895&tool=pmcentrez&rendertype=abstract

[3] A. C. Ho *et. al.*, "Long-term results from an epiretinal prosthesis to restore sight to the blind," *Ophthalmology*, vol. 122, no. 8, pp. 1547–1554, 2015. [Online]. Available: http://dx.doi.org/10.1016/j.ophtha.2015.04.032

[4] A. C. Weitz *et al.*, "Interphase gap as a means to reduce electrical stimulation thresholds for epiretinal prostheses," *J. Neural Eng.*, vol. 11, no. 1, pp. 1–9, 2014.

[5] A. E. Hadjinicolaou *et al.*, "Optimizing the electrical stimulation of retinal ganglion cells," *IEEE Trans. Neural Syst. Rehabil. Eng.*, vol. 23, no. 2, pp. 169–178, Mar. 2015.

[6] S. I. Fried, H. A. Hsueh, and F. S. Werblin, "A method for generating precise temporal patterns of retinal spiking using prosthetic stimulation," *J. Neurophysiol.*, vol. 95, no. 2, pp. 970–978, 2005. [Online]. Available: http://jn.physiology.org/content/95/2/970.full

[7] K. Loizos, G. Lazzi, R. Marc, and C. Cela, "Virtual electrode design for increasing spatial resolution in retinal prosthesis," *Healthcare Technol. Lett.*, vol. 3, no. 2, pp. 93–97, 2016. [Online]. Available: http://digital-library.theiet.org/content/journals/10.1049/htl.2015.0043

[8] L. H. Jepson *et al.*, "Spatially patterned electrical stimulation to enhance resolution of retinal prostheses," *J. Neurosci.*, vol. 34, no. 14, pp. 4871–4881, 2014.

[9] G. K. Moghaddam, N. H. Lovell, R. G. Wilke, G. J. Suaning, and S. Dokos, "Performance optimization of current focusing and virtual electrode strategies in retinal implants," *Comput. Methods Programs Biomed.*, vol. 117, no. 2, pp. 334–342, 2014.

[10] D. K. Freeman, J. S. Jeng, S. K. Kelly, E. Hartveit, and S. I. Fried, "Calcium channel dynamics limit synaptic release in response to prosthetic stimulation with sinusoidal waveforms," *J. Neural Eng.*, vol. 8, no, 4, p. 046005, 2011.

[11] D. K. Freeman, D. K. Eddington, J. F. Rizzo III, S. I. Fried, and J. F. Rizzo, "Selective activation of neuronal targets with sinusoidal electric stimulation," *J. Neurophysiol.*, vol. 104, no. 5, pp. 2778–2791, 2010.

[12] P. Twyford, C. Cai, and S. Fried, "Differential responses to high-frequency electrical stimulation in ON and OFF retinal ganglion cells," *J. Neural Eng.*, vol. 11, no. 2, p. 025001, 2014. [Online]. Available: http://www.ncbi.nlm.nih.gov/pubmed/24556536

[13] T. Guo *et al.*, "Selective activation of ON and OFF retinal ganglion cells to high-frequency electrical stimulation: A computational modeling study," in *Proc. 36th Annu. Int. Conf. IEEE Eng. Med. Biol. Soc.*, Aug. 2014, pp. 6108–6111. [Online]. Available: http://ieeexplore.ieee.org/xpls/abs_all.jsp?arnumber=6945023

[14] L. H. Jepson *et al.*, "Focal electrical stimulation of major ganglion cell types in the primate retina for the design of visual prostheses," *J. Neurosci.*, vol. 33, no. 17, pp. 7194–7205, 2013. [Online]. Available: http://www.ncbi.nlm.nih.gov/pubmed/23616529

[15] M. R. Behrend, A. K. Ahuja, M. S. Humayun, R. H. Chow, and J. D. Weiland, "Resolution of the epiretinal prosthesis is not limited by electrode size," *IEEE Trans. Neural Syst. Rehabil. Eng.*, vol. 19, no. 4, pp. 436–442, Aug. 2011.

[16] H. Kasi, W. Hasenkamp, G. Cosendai, A. Bertsch, and P. Renaud, "Simulation of epiretinal prostheses—Evaluation of geometrical factors affecting stimulation thresholds," *J. Neuroeng. Rehabil.*, vol. 8, no. 1, p. 44, 2011. [Online]. Available: http://www.ncbi.nlm.nih.gov/pubmed/21854602

[17] M. A. Schiefer and W. M. Grill, "Sites of neuronal excitation by epiretinal electrical stimulation," *IEEE Trans. Neural Syst. Rehabil. Eng.*, vol. 14, no. 1, pp. 5–13, Mar. 2006.

[18] D. Tsai, S. Chen, D. A. Protti, J. W. Morley, G. J. Suaning, and N. H. Lovell, "Responses of retinal ganglion cells to extracellular electrical stimulation, from single cell to population: model-based analysis," *PLoS ONE*, vol. 7, no. 12, p. e53357, 2012.

[19] T. M. O'Hearn, S. R. Sadda, J. D. Weiland, M. Maia, E. Margalit, and M. S. Humayun, "Electrical stimulation in normal and retinal degeneration (rd1) isolated mouse retina," *Vis. Res.*, vol. 46, no. 19, pp. 3198–3204, 2006.

[20] S. Suzuki *et al.*, "Comparison of electrical stimulation thresholds in normal and retinal degenerated mouse retina," *Jpn. J. Ophthalmol.*, vol. 48, no. 4, pp. 345–349, 2004.

[21] R. J. Jensen and J. F. Rizzo, "Activation of retinal ganglion cells in wild-type and rd1 mice through electrical stimulation of the retinal neural network," *Vis. Res.*, vol. 48, no. 14, pp. 1562–1568, 2008.

[22] R. J. Jensen and J. F. Rizzo III, "Activation of ganglion cells in wild-type and rd1 mouse retinas with monophasic and biphasic current pulses," *J. Neural Eng.*, vol. 6, no. 3, p. 035004, 2009.

[23] R. J. Jensen, "Activation of ganglion cells in wild-type and P23H rat retinas with a small subretinal electrode," *Experim. Eye Res.*, vol. 99, pp. 71–77, Jun. 2012.

[24] C. Sekirnjak *et al.*, "Loss of responses to visual but not electrical stimulation in ganglion cells of rats with severe photoreceptor degeneration," *J. Neurophysiol.*, vol. 102, no. 6, pp. 3260–3269, 2009.

[25] C. Sekirnjak *et al.*, "Changes in physiological properties of rat ganglion cells during retinal degeneration," *J. Neurophysiol.*, vol. 105, no. 5, pp. 2560–2571, 2011.

[26] A. C. Weitz *et al.*, "Improving the spatial resolution of epiretinal implants by increasing stimulus pulse duration," *Sci. Transl. Med.*, vol. 7, no. 318, p. 318ra203, Dec. 2015.

[27] B. W. Jones *et al.*, "Retinal remodeling in the Tg P347l rabbit, a large-eye model of retinal degeneration," *J. Comparative Neurol.*, vol. 519, no. 14, pp. 2713–2733, Oct. 2011.

[28] K. Loizos, G. Lazzi, J. Lauritzen, J. Anderson, B. Jones, and R. Marc, "A multi-scale computational model for the study of retinal prosthetic stimulation," in *Proc. 36th Annu. Int. Conf. IEEE Eng. Med. Biol. Soc.*, Aug. 2014, pp. 6100–6103.

[29] M. Abramian, N. H. Lovell, J. W. Morley, G. J. Suaning, and S. Dokos, "Activation and inhibition of retinal ganglion cells in response to epiretinal electrical stimulation: A computational modelling study," *J. Neural Eng.*, vol. 12, no. 1, pp. 1–17, 2015. [Online]. Available: http://www.ncbi.nlm.nih.gov/pubmed/25426958

[30] B. W. Jones *et al.*, "Retinal remodeling triggered by photoreceptor degenerations," *J. Comparative Neurol.*, vol. 464, no. 1, pp. 1–16, 2003.

[31] B. W. Jones, R. L. Pfeiffer, W. D. Ferrell, C. B. Watt, J. Tucker, and R. E. Marc, "Retinal remodeling and metabolic alterations in human AMD," *Frontiers Cellular Neurosci.*, vol. 10, P. 103, Apr. 2016.

[32] R. Marc, B. Jones, C. B. Watt, and E. Strettoi, "Neural remodeling in retinal degeneration," *Prog. Retinal Eye Res.*, vol. 22, no. 5, pp. 607–655, Sep. 2003.

[33] A. H. Toychiev, E. Ivanova, C. W. Yee, and B. T. Sagdullaev, "Block of gap junctions eliminates aberrant activity and restores light responses during retinal degeneration," *J. Neurosci.*, vol. 33, no. 35, pp. 13972–13977, 2013.

[34] D. J. Margolis and P. B. Detwiler, "Cellular origin of spontaneous ganglion cell spike activity in animal models of retinitis pigmentosa," *J. Opthalmol.*, vol. 2011, pp. 1–6, 2011, Art. no. 507037.

[35] S. Trenholm and G. B. Awatramani, "Origins of spontaneous activity in the degenerating retina," *Frontiers Cellular Neurosci.*, vol. 9, no. 277, pp. 1–7, 2015. [Online]. Available: http://journal.frontiersin.org/article/10.3389/fncel.2015.00277/abstract

[36] J. Borowska, S. Trenholm, and G. B. Awatramani, "An intrinsic neural oscillator in the degenerating mouse retina," *The J. Neurosci., Off. J. Soc. Neurosci.*, vol. 31, no. 13, pp. 5000–5012, 2011.

[37] H. Choi *et al.*, "Intrinsic bursting of AII amacrine cells underlies oscillations in the rd1 mouse retina," *J. Neurophysiol.*, vol. 112, no. 6, pp. 1491–1504, 2014. [Online]. Available: http://www.ncbi.nlm.nih.gov/pubmed/25008417

[38] A. Cho, C. Ratliff, A. Sampath, and J. Weiland, "Changes in ganglion cell physiology during retinal degeneration influence excitability by prosthetic electrodes," *J. Neural Eng.*, vol. 13, no. 2, p. 025001, 2016.

[39] Y. S. Goo, D. J. Park, J. R. Ahn, and S. S. Senok, "Spontaneous oscillatory rhythms in the degenerating mouse retina modulate retinal ganglion cell responses to electrical stimulation," *Frontiers Cellular Neurosci.*, vol. 9, p. 512, Jan. 2016.

[40] D. Park, S. Senok, and Y. Goo, "Degeneration stage-specific response pattern of retinal ganglion cell spikes in rd10 mouse retina," in *Proc. 37th Annu. Int. Conf. IEEE Eng. Med. Biol. Soc. (EMBC)*, Aug. 2015, pp. 3351–3354.

[41] C. J. Cela, "A multiresolution admittance method for large-scale bioelectromagnetic interactions," Ph.D. dissertation, Dept. Elect. Eng., North Carolina State Univ., Raleigh, NC, USA, 2010.

[42] N. T. Carnevale and M. L. Hines, *The Neuron Book*. Cambridge, UK: Cambridge Univ. Press, 2006.

[43] K. Loizos, A. K. RamRakhyani, J. Anderson, R. Marc, and G. Lazzi, "On the computation of a retina resistivity profile for applications in multi-scale modeling of electrical stimulation and absorption," *Phys. Med. Biol.*, vol. 61, no. 12, pp. 4491–4505, 2016.

[44] C. J. Cela, R. C. Lee, and G. Lazzi, "Modeling cellular lysis in skeletal muscle due to electric shock," *IEEE Trans. Biomed. Eng.*, vol. 58, no. 5, pp. 1286–1293, May 2011.

[45] R. E. Marc, B. W. Jones, C. B. Watt, J. R. Anderson, and C. Sigulinsky, "Retinal connectomics: Towards complete, accurate networks," *Prog. Retinal Eye Res.*, vol. 37, pp. 141–162, Nov. 2013.

[46] C. Gabriel, "Compilation of the dielectric properties of body tissues at RF and microwave frequencies," Occupational Environ. Health Directorate, Radiofreq. Radiat. Division, Brooks Air Force Base, San Antonio, TX, USA, Tech. Rep. N.AL/OE-TR-1996-0037, 1996.

[47] H. Cheng *et al.*, "Structural and functional MRI reveals multiple retinal layers," *Proc. Nat. Acad. Sci. USA*, vol. 103, no. 46, p. 17525–17530, 2006.

[48] J. R. Anderson *et al.*, "Exploring the retinal connectome," *Mol. Vis.*, vol. 17, pp. 355–379, Feb. 2011. [Online]. Available: http://www.ncbi.nlm.nih.gov/pubmed/21311605

[49] J. F. Fohlmeister and R. F. Miller, "Impulse encoding mechanisms of ganglion cells in the tiger salamander retina," *J. Neurophysiol.*, vol. 78, no. 4, pp. 1935–1947, 1997.

[50] J. F. Fohlmeister, E. D. Cohen, and E. A. Newman, "Mechanisms and distribution of ion channels in retinal ganglion cells: Using temperature as an independent variable," *J. Neurophysiol.*, vol. 103, no. 3, pp. 1357–1374, 2010. [Online]. Available: http://www.ncbi.nlm.nih.gov/pubmed/20053849

[51] S. Usui, A. Ishihaiza, Y. Kamiyama, and H. Ishii, "Ionic current model of bipolar cells in the lower vertebrate retina," *Vis. Res.*, vol. 36, no. 24, pp. 4069–4076, Dec. 1996.

[52] R. Publio, R. F. Oliveira, and A. C. Roque, "A computational study on the role of gap junctions and rod Ih conductance in the enhancement of the dynamic range of the retina," *PLoS ONE*, vol. 4, no. 9, p. e6970, 2009.

[53] M. A. Sikora, J. Gottesman, and R. F. Miller, "A computational model of the ribbon synapse," *J. Neurosci. Methods*, vol. 145, nos. 1–2, pp. 47–61, Jun. 2005.

[54] M. Mahadevappa, J. D. Weiland, D. Yanai, I. Fine, R. J. Greenberg, and M. S. Humayun, "Perceptual thresholds and electrode impedance in three retinal prosthesis subjects," *IEEE Trans. Neural Syst. Rehabil. Eng.*, vol. 13, no. 2, pp. 201–206, Jun. 2005.

[55] R. E. Marc, J. R. Anderson, B. W. Jones, C. L. Sigulinsky, and J. S. Lauritzen, "The aii amacrine cell connectome: A dense network hub," *Frontiers Neural Circuits*, vol. 8, p. 104, Sep. 2015.

[56] R. Publio, C. C. Ceballos, and A. C. Roque, "Dynamic range of vertebrate retina ganglion cells: Importance of active dendrites and coupling by electrical synapses," *PLoS ONE*, vol. 7, no. 10, p. e48517, 2012.

[57] R. V. Shannon, "A model of safe levels for electrical stimulation," *IEEE Trans. Biomed. Eng.*, vol. 39, no. 4, pp. 424–426, Apr. 1992.

[58] D. B. McCreery, W. F. Agnew, T. G. H. Yuen, and L. Bullara, "Charge density and charge per phase as cofactors in neural injury induced by electrical stimulation," *IEEE Trans. Biomed. Eng.*, vol. 37, no. 10, pp. 996–1001, Oct. 1990.

[59] D. R. Merrill, M. Bikson, and J. G. R. Jefferys, "Electrical stimulation of excitable tissue: Design of efficacious and safe protocols," *J. Neurosci. Methods*, vol. 141, no. 2, pp. 171–198, 2005.

[60] H. Hoshi, L.-M. Tian, S. C. Massey, and S. L. Mills, "Two distinct types of on directionally selective ganglion cells in the rabbit retina," *J. Comparative Neurol.*, vol. 519, no. 13, pp. 2509–2521, 2011.

[61] R. L. Pfeiffer, R. E. Marc, M. Kondo, H. Terasaki, and B. W. Jones, "Müller cell metabolic chaos during retinal degeneration," *Experim. Eye Res.*, vol. 150, pp. 62–70, Sep. 2016.

[62] K. N. Ahn *et al.*, "Effect of stimulus waveform of biphasic current pulse on retinal ganglion cell responses in retinal degeneration (rd1) mice," *The Korean J. Physiol. Pharmacol.*, vol. 19, no. 2, pp. 167–175, 2015.